Journal Pre-proof

A new miniaturised short-wave infrared (SWIR) spectrometer for on-site cultural heritage investigations

Emilio Catelli, Giorgia Sciutto, Silvia Prati, Marco Valente Chavez Lozano, Lucrezia Gatti, Federico Lugli, Sara Silvestrini, Stefano Benazzi, Emiliano Genorini, Rocco Mazzeo

PII: S0039-9140(20)30403-3

DOI: https://doi.org/10.1016/j.talanta.2020.121112

Reference: TAL 121112

To appear in: *Talanta*

Received Date: 3 March 2020

Revised Date: 28 April 2020

Accepted Date: 30 April 2020

Please cite this article as: E. Catelli, G. Sciutto, S. Prati, M.V. Chavez Lozano, L. Gatti, F. Lugli, S. Silvestrini, S. Benazzi, E. Genorini, R. Mazzeo, A new miniaturised short-wave infrared (SWIR) spectrometer for on-site cultural heritage investigations, *Talanta* (2020), doi: https://doi.org/10.1016/j.talanta.2020.121112.

CREDIT AUTHOR STATEMENT

Emilio Catelli: Investigation, Data curation, Writing- Original draft preparation.

Giorgia Sciutto: Conceptualization, Methodology, Writing - Review & Editing, Supervision.

Silvia Prati: Writing - Review & Editing, Validation

Marco Valente Chavez Lozano: Investigation, Writing- Original draft preparation.

Lucrezia Gatti: Investigation, Writing- Original draft preparation.

Federico Lugli: Resources, Writing- Original draft preparation.

Sara Silvestrini: Resources.

Stefano Benazzi: Writing - Review & Editing

Emiliano Genorini: Resources, Writing - Review & Editing

Rocco Mazzeo: Writing - Review & Editing

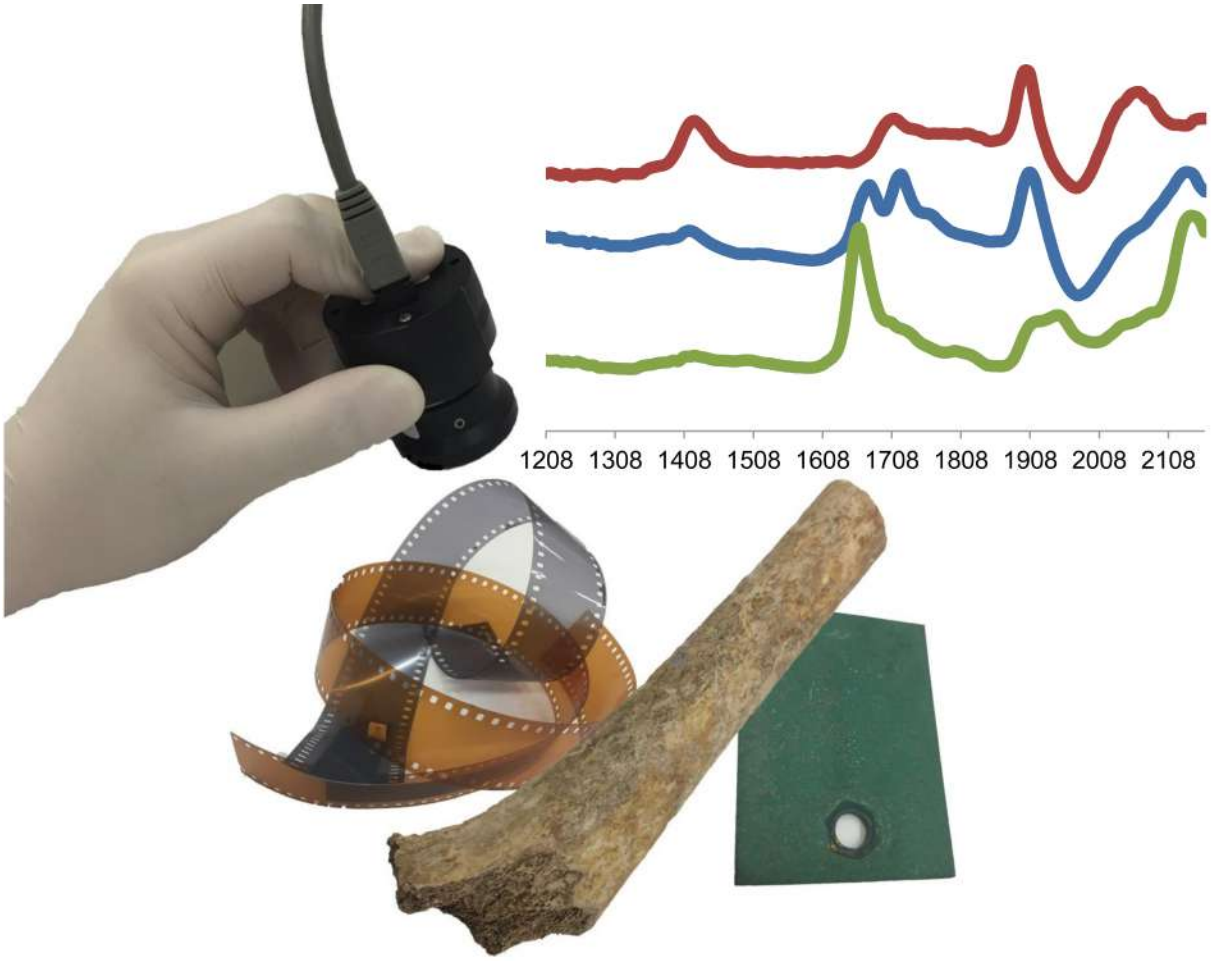

A NEW MINIATURISED SHORT-WAVE INFRARED (SWIR) SPECTROMETER FOR ON-SITE CULTURAL HERITAGE INVESTIGATIONS

Emilio Catelli[1], Giorgia Sciutto[1]*, Silvia Prati[1], Marco Valente Chavez Lozano[1], Lucrezia Gatti[1], Federico Lugli[2], Sara Silvestrini[2], Stefano Benazzi[2], Emiliano Genorini[3], Rocco Mazzeo[1]

[1]University of Bologna, Department of Chemistry "G. Ciamician", Ravenna Campus, Via Guaccimanni, 42 – 48121 Ravenna, Italy

[2]University of Bologna, Department of Cultural Heritage, Ravenna Campus, Via degli Ariani, 1 – 48121 Ravenna, Italy

[4]Viavi Solutions, Via Enrico Cernuschi 8 – 20900 Monza, Italy

*Corresponding author.
e-mail address: giorgia.sciutto@unibo.it;
phone number: +39 0544 937155

Abstract

The paper reports on the development of an analytical method based on the use of a new miniaturised short-wave infrared (SWIR) spectrometer for the analysis of cultural heritage samples. The spectrometer is a prototype characterised by small dimension (45.0 mm in diameter x 47.5 mm in height x 60 grams weight), easily handled and transferable out of research laboratories. The prototype enables the acquisition of spectra in the SWIR range of 1200 – 2200 nm, which is a unique feature for miniaturised spectrometers. The exploitation of this spectral range allows the detection of a high number of combination and overtone bands, which guarantees significant diagnostic power to the instrument. The present study lays a significant foundation to the development of analytical strategies based on miniaturised NIR spectrometers working in the SWIR spectral range for the characterization of complex samples such as cultural heritage specimens. Analytical performances of the new spectrometer were assessed on archaeological bones, cinematographic films and bronze patinas. The selected cases of study present challenging conservation issues not properly addressed, and their analyses usually require to be performed on-site, in places not easily accessible by restorers, archaeologists and/or scientists. The data acquired with the prototype, combined with a multivariate data analysis approach, show the possibility to i) differentiate between the materials used as a support for cinematographic film namely cellulose nitrate (CN), cellulose acetates (CA) and polyethylene terephthalate (PET); ii) sort out archaeological bone fragments according to their collagen content as an initial screening test for bones characterization; iii) differentiate between corrosion products on outdoor bronze sculpture, which is important for assessing the state of conservation of the artwork. The prototype enabled rapid information acquisition to guide restoration strategies, which need to be supported in real time by quick and easy analytical procedures.

Keywords

Miniaturised palm-sized spectrometer; Short-wave infrared (SWIR) spectroscopy; On-site investigations; Archaeological bones; Cinematographic films; Bronze patinas.

1. Introduction

The miniaturization of vibrational spectrometers and sensors has revolutionised the analytical field and has led to portability, simplified use through automation, and the reduction in time and costs of the analyses [1]. These advantages have attracted interest from end-users and product developers for on-site and on-line analytical applications. Miniaturised spectrometers represent a new generation of portable diagnostic systems [2], which can be associated with automatic data processing methods, leading to an easy interpretation of the results even by non-specialist technicians. Near infrared (NIR) spectrometers are used for developing miniaturised analytical tools: no sample preparation is required, and measurements are usually fast and completely non-invasive [3]. NIR spectrometers have already been widely used in industry for quality control via data processing methods. In addition, miniaturised NIR spectrometers have been applied in agro-food [4, 5] and pharmaceutical research [6, 7], as well as in diagnostic studies in forensic fields [8].

Miniaturised NIR spectrometers could also represent a turning point in the chemical investigation of the cultural heritage. Although the importance of scientific analyses in the conservation field is largely acknowledged, the related cost, time and expertise required are often not feasible.

In cultural heritage research, the use of NIR spectroscopy (1000 – 2500 nm) has had a late and slow introduction, with respect to other research fields. Nevertheless, in the last decades NIR spectrometry has moved from laboratory benchtop instruments to portable devices that can be used on-site, attracting an increasing interest for the non-invasive study of works of art in galleries or museums, without requiring precious objects to be moved or sampled.

NIR molecular investigation has been carried out on stones [9], paintings [10] and illuminated manuscript [11, 12] using optical fibre spot reflectance spectroscopy. The spectral range used for the single point analysis varies according to the type of sensor spectrometer used, typically: 400-1000 nm (Visible-NIR range), 780-1000 (NIR range), 1050-1700 nm and 1050-2500 nm (Short-Wave-IR ranges) [13]. More recently, research has also focused on NIR hyperspectral imaging which provides chemical images, simultaneously obtaining information on the molecular composition and spatial distribution of the constituents [14, 15].

In this paper we assess the potential of a new miniaturised SWIR prototype for the qualitative investigation of artistic and archaeological objects, for on-site use (Fig. 1). The prototype is very small (45 mm in diameter x 47.5 mm in height), weighs very little (60 grams) and uses a simple method based on bringing the sensor into contact with the surface to be analysed. The prototype exploits a SWIR range of 1200 – 2200 nm, presenting a unique feature for miniaturised NIR devices which usually have a limited range between 900-1700 nm [16-18]. The analysis guarantees the good diagnostic power of the data in heterogeneous artwork samples, exploiting a spectral range characterized by a high number of combination and overtone bands [19].

We believe that this is the first time that a miniaturised NIR spectrometer working in the SWIR spectral range has been proposed for the characterization of cultural heritage materials.

Challenging conservation issues were considered in an attempt to address new specific needs and conservation issues that to date have not been studied sufficiently. Archaeological bones,

cinematographic films and bronze patinas were investigated. All our case studies were linked to particular needs: the analysis had to be performed on-site (archaeological excavations, film restoration laboratories, and sites of monuments) and to be carried out in places that were not easily accessible (scaffolding, isolated places) by restorers, archaeologists and/or scientists. The NIR prototype enabled rapid information acquisition to guide restoration strategies, which needed to be supported in real time by quick and easy analytical procedures. We thus implemented appropriate reflectance spectral databases and tailored-data processing methods for the identification of the materials.

2. Materials and Methods

2.1 Miniaturised NIR spectrometer and data elaboration

The NIR prototype was designed by Viavi Solutions (JDSU Corporation, Milpitas, CA) (Fig. 1) [5, 6]. The system measures the diffuse reflectance in the spectral region of 1208–2160.5 nm (8278–4629 cm^{-1}). It is controlled by a portable computer via USB port. A linear-variable filter (LVF) is used as the dispersing element. LVF is directly connected to a 128-pixel linear Indium Gallium Arsenide (InGaAs) uncooled detector, which results in a compact device. Two tungsten light bulbs were used as the radiation source. The spot of analysis is approximately 3 mm in diameter. All the collected spectra were recorded nominal spectral at a nominal resolution of 7.68 nm. Spectralon was used as the NIR-reflectance standard with 99% diffuse reflectance. The spectrum acquisition was performed with an integration time of 3 ms and 1000 scans resulting in a measurement time of 3 s per sample. The MicroNIR Pro software (JDSU Corporation, Milpitas, CA) was used for data acquisition.

Multivariate data processing was performed by means of in-house Matlab routines (The Mathworks Inc., Natick, USA). Suitable row pre-treatments were selected and applied in attempt to minimise systematic unwanted variations, which could affect the signals. In more details, standard normal variate (SNV) transform was selected to correct for both baseline shifts and global intensity variations, while first Savitzky-Golay derivation was applied to enhance details within complex spectral features (e.g. unresolved broad shape bands). Afterwards, the spectra range considered were the following: 1369.3-2122.1 nm for cinematographic films, 1254.9- 2122.1 nm for bone samples and 1307.9-2091.4 nm for copper-based corrosion products. Column centring was performed prior to principal component analysis (PCA).

2.2 Cinematographic films

A total of 79 developed cinematographic film rolls or roll sections characterised by different polymeric bases (cellulose nitrate -CN-, cellulose acetates -CA- and polyethylene terephthalate PET) were analyzed. Samples belonged to different typologies (Black and white, Colour, Negative, Positive and intermediate elements) and manufacturing companies (Eastman Kodak©, Agfa©, 3M©, Ferrania©, Pathe©, Orwo© and Fuji©). Preliminary information about the polymeric base composition was obtained by films inscriptions and conventional mechanical and visual films examination. According to their state of conservation film samples were broadly grouped in “well-preserved” (10 CN samples, 19 CA samples, and 13 PET samples) and “degraded” (16 CN samples, 11 CA samples, and 10 PET samples).

At least 5 spectra from each sample were recorded by placing the film between the spectrometer and the gold-coated glass holder. All films were analyzed directly in contact with the polymeric base.

2.3 Ancient Bones

A total of 7 bone samples coming from different Italian archaeological sites (Table 1) were analysed. Samples were selected based on their ages (from ca. 45 ka to Early modern times) and provenances (from Southern to Northern Italy). Most of them (RB63, R313, UC86, UC88) are undetermined bone fragments of animal origin, while two bones (RP and SMM) belonged to *Homo sapiens*. Sample OV is attributable to an ovicaprid. Bone samples are characterized by different state of conservation, according to the excavation site and age. On these bases it was possible to argue that samples RP, SMM and OV could present a higher collagen content in comparison to samples RB and to those from Uluzzo archaeological site.

Table 1: Bone samples investigated

Sample	**Provenance**	**Date**	**Species**	**Anatomy**	**Notes**
RP	Roccapelago (Modena, Italy)	16th-18th cent.	Homo sapiens	femur section	Partially mummified individual
SMM	Santa Maria Maggiore (Trento, Italy)	15th cent.	Homo sapiens	talus	-
OV	Ostra Vetere (Ancona, Italy)	6th-7th cent.	Ovicaprid	tibia	-
RB63	Riparo Broion (Vicenza, Italy)	45 ka	undetermined/fauna	bone fragment	-
R313	Uluzzo C (Nardò, Italy)	42 ka	undetermined/fauna	bone fragment	badly preserved
UC86	Uluzzo C (Nardò, Italy)	42 ka	undetermined/fauna	bone fragment	badly preserved
UC88	Uluzzo C (Nardò, Italy)	42 ka	undetermined/fauna	bone fragment	badly preserved

A total of 11 spectra were recorded for each sample, positioning the sensor directly in contact with the bone surface.

2.4 Copper-based corrosion products

Brochantite ($Cu_4SO_4(OH)_6$), antlerite ($Cu_3SO_4(OH)_4$), and atacamite ($Cu_2Cl(OH)_3$) were synthesized in laboratory and characterized by XRD and FTIR spectroscopy, in order to have pure standard reference materials. The analysis of the standards was performed by positioning the instrument on pressed pellets made of 200 mg of pure compound [20]. Eleven spectra were recorded for each sample.

Copper and bronze plates (5 x 7 cm) naturally and artificially aged have been selected as representative samples of outdoor bronze patinas. All samples show similar stratigraphy represented by a brown layer of cuprite adherent to the metal/alloy and an external layer of green copper hydroxysalts on top of the cuprite layer. The urban natural sample (UN) is characterised by the presence of a thin layer of cuprite and brochantite produced on a copper plate coming from a roof which has been exposed to the urban atmosphere of Munich (Germany) for almost 80 years; the natural patina was further subjected to artificial ageing under UV radiation [21] and salt exposure [22] for a total of 2000 hours. The urban artificial patina (UA) was artificially generated by employing the Pichler process, which allows to create an external green thick layer of copper hydroxysulphate brochantite. Antlerite was observed in the UA patina as well, in minor amount compared to brochantite [23]. The UA sample was submitted to the same artificial ageing process previously described for the UN sample. The marine natural (MN) sample, is characterised by the presence of an external layer of atacamite with phosphates, silicates and malachite in minor amount and was obtained exposing samples to the marine environment of Cabo Raso (Portugal) for 31 months. The patina components of UN, UA and MN samples were characterized by XRD and FTIR analysis [24]. The analysis was performed by placing the spectrometer in contact with the patina. Eleven spectra were recorded for each sample.

3. Results and Discussion

3.1 Historical cinematographic films

In general terms, cinematographic films are made up of a thick, transparent polymeric base, which supports the thinner sub-layers that contain the recorded image and/or sound. Three general types of materials are used to produce the bases for film: cellulose nitrate (CN), cellulose acetates (CA), and polyethylene terephthalate (PET). CN and CA film bases are intrinsically unstable, tending to lose their acetyl and nitro functional groups via hydrolysis [25, 26]. Such phenomena, together with the decomposition of gelatine and the plasticizer migration, are the most important causes of cinematographic film degradation. To slow down the film's degradation rate, controlled storing conditions need be adopted, according to the type of polymeric base (such as the freezing of CN elements). However, this may drastically increase the cost of the conservation of film collections. Thus, accurate identification of the film base is important for the most rational resource management of a movie archive.

The traditional approach to identifying film bases consists in a simple visual examination of the film's inscriptions and an empirical assessment of its structural characteristics. However, this can sometimes lead to an erroneous identification. Chromatographic techniques have also been proposed for characterizing the polymers used both in animation cels and cinematographic films [27, 28]. However, chromatographic analyses in most cases are costly, long, and require complex instrumentation and reagents, and they are invasive, requiring samples [29]. In comparison, spectroscopic analyses are a simpler and more accessible way to characterize film and animation cel bases: Raman spectroscopy [25, 30], FTIR spectroscopy in transmission and Attenuated Total Reflection (ATR) modes [27, 30, 31] and NIR spectroscopy have been proposed. However, these techniques involve several drawbacks such as the non-portability of the instruments, the danger of damaging the sample during the analysis, or the occurrence of fluorescence in Raman spectra.

Portable NIR sensors are a promising alternative for film base studies, as they require much less analysis time and less expensive instruments. They can also be used on-site in a completely non-invasive way.

In order to offer a suitable diagnostic tool for film base identification, the performance of our new NIR prototype system was evaluated. Spectra of the three classes of polymers used as film bases showed particular spectral profiles in the NIR region of between 1200 and 2200 nm, which enabled them to be identified (Table2, Fig. 2a).

Table 2: Absorption bands in the NIR region of cellulose nitrate (CN), cellulose acetates (CA) and polyethylene (PE).

Cellulose nitrate (nm)	**Cellulose acetate (nm)**	**Polyethylene (nm)**	**Tentative Assignment**
1423	1415		1st overtone of OH stretching [32-34]
		1415	1st overtone of OH stretching [35]
	1677	1661	1st overtone of CH stretching [35-39]
1707	1723	1707	1st overtone of CH stretching [34, 35, 40, 41]
		1799	-
1899			1st combination of OH stretching and bending [40]
	1907	1915	1st combination of OH stretching and bending [32, 40, 42], 2nd overtone C=O stretching [34, 35, 43]
		1945	2nd overtone of C=O stretching [42, 44]
2021			-
	2137	2137	Combination band of aromatic CH stretching and ring vibration [42]

CN features diagnostic bands at 1423 nm (1st overtone of OH stretching), and at 1707 nm (1st overtone of CH stretching) [39]. CA samples can be easily identified and differentiated from the nitrocellulose-based films due to the characteristic double band at 1677 nm (1st overtone stretching of CH)[39] and at 1723 nm (1st overtone of CH stretching) [41]. Finally, the different chemical nature of PE bases led to a NIR spectrum that was very dissimilar from the previous ones and characterised by a very strong band at 1661 nm that can be attributed to the 1st overtone of CH stretching [37]. PE spectra were also characterised by a band at 2138 nm due to the combination band of aromatic CH stretching and ring vibration [42].

This simple identification of the diagnostic band thus differentiates among the film bases. The data obtained were processed with principal component analysis (PCA) in order to assess the robustness and the discriminatory power of the method. Chemometric tools may also enable simple analysis

methods to be developed that can support conservators and archive staff in interpreting the results. The resulting score scatter plot clearly shows three different clusters associated with the three classes of cinematographic film bases (Fig. 2c). The interpretation of the loadings scatter plots (Fig. 2d) enables the variables involved in the sample separation to be clearly identified. The diagnostic bands at 1423 and 1707 nm (in the loading plot variables at around 1690 nm and 1400 nm related to bands after derivative correction) played a crucial role in the separation of CN samples, as expected. On the other hand, CA samples were characterised by bands at 1723 and 1907 nm (variables around 1707 and 1892 related to bands after derivative correction), while the PE basis can be clustered thanks to the presence of bands at 1661 and at 2138 nm (corresponding to bands with a derivative-like shape at about 1638 and 2114 nm).

The correct identification of film bases is even more important in degraded and partially altered films, which usually require urgent conservation actions together with appropriate storage. The performance of the micro NIR prototype was therefore also evaluated on degraded samples belonging to the three different classes. Degraded films are characterized by a reduced mechanical resistance, embrittlement, distortion and shrinkage, dye plasticizer exudation, dye fade, gelatine decomposition, delamination and “channelling” of the emulsion [45].

Spectra collected from CA degraded samples showed a strong decrease in the bands at 1661 and at 1723 nm. Conversely, a broad band appeared at 1462 nm which was attributed to the 1st overtone of free OH (Fig. 3a). These outcomes may be related to the hydrolytic degradation observed in CA degraded materials [46]. To test the discrimination ability of the unsupervised model, a new dataset was created, including both well-preserved and degraded samples, and then submitted to PCA. The resulting plot described three main clusters associated with the three different types of polymers, each containing well-preserved and degraded samples (Fig. 3c). The limited dispersion of samples belonging to the same class led to a good discrimination among the various polymeric classes. The loadings plot (Fig. 3d) confirmed the diagnostic role of bands at 1661, 1707, 1723 and 2138 nm, as previously described. Our NIR prototype is thus suitable for the identification of the film support irrespectively of the state of conservation.

3.2 Ancient Bones

The characterization of bone proteins in human and animal remains is fundamental for phylogenetic and diagenetic studies of ancient populations. Collagen is the main protein in bone, with non-collagenous proteins (NCPs) being less abundant. Proteomic, radiocarbon and stable isotope analyses of bones, can provide information on the taxonomy, age, diet and mobility of ancient populations. Unfortunately, the effectiveness of these investigations can be compromised if the amount of preserved collagen is too low [47-49]. In fact, collagen is subject to significant alterations mostly due to changes in the climate and the burial environment [50]. The above-mentioned analyses are therefore usually performed on a very large number of samples, with a high cost in terms of time and money.

Rapid screening methods are thus increasingly employed to detect collagen in bones before the bones are subjected to further analyses. Bone samples can be investigated through elemental analyses for the evaluation of the %N content [49]. Raman and Fourier-transformed infrared spectroscopy have also been proposed as screening tools for the detection of collagen in bones, with the use of microscopes and bench instruments [51-53] as well as portable instrumentation [54, 55].

However, these analytical approaches are destructive and/or time consuming, limiting their application to large numbers of bone samples.

NIR has been applied for taxonomical discrimination of bones [56] as well as for the non-invasive evaluation of bone preservation. Bone collagen is detected thanks to the presence of diagnostic proteinaceous bands in the NIR spectral region [57-59]. To date bones samples have mainly been analysed in the laboratory with benchtop spectrometers. A portable NIR spectrometer coupled with fibre-optic reflectance probe was recently tested for in situ analyses [60]. Our new miniaturized device, which is inexpensive and easier to use than conventional portable spectrometers, appears to have great potential as a screening tool for use in situ during archeological excavations.

To evaluate the performance of our NIR device, we analysed seven bone samples, from two archaeological sites and characterized by different conservation stories (Table 1). We speculated a higher collagen content (%) for specimen RP (partially mummified individual) and a lower content for the Palaeolithic samples (RB63, R313, UC86 and UC88; <1%). Although older in terms of absolute age, macroscopically sample RB63 appears to be better preserved than the Uluzzo samples (R313, UC86 and UC88). This may be related to the different burial environments of the two places. RB63 comes from the northern site of the Riparo Broion (Vicenza, Italy), which has a lower annual temperature than Uluzzo. Samples OV and SMM, from the Late Antiquity and Late Medieval periods respectively, should present a collagen content that is somewhere between the content found in Palaeolithic and modern specimens.

Our preliminary hypotheses were in line with the observations of the spectra profiles (Fig. 4a), which enabled us to identify the collagen diagnostic band at 2053 nm (N-H combination bands) in four samples: RP, SMM, OV and RB63. A shoulder band was also identified at about 1692 nm likely due to the first overtone C-H stretching (better visible after the first derivative correction with a band at 1677 nm) in sample RP, SMM, OV. On the other hand, for the other samples (Uluzzo), no evidence of collagen was found either in the raw data or in the spectra after the first derivative correction, which is commonly applied to increase the readability and identification of weak and broad NIR bands.

The PC1 vs PC3 score plot showed an appreciable separation of the samples (Fig. 4c). Spectra obtained on RP, SMM, OV and RB63 samples showed a good reproducibility leading to a low dispersion in the scatter plot. Conversely, samples R313, UC86, UC88 were characterized by a higher dispersion, making a clear separation between them difficult. The analysis of the loadings plot (Fig. 4d) indicated the crucial role played by the band at 2053 nm (2022 nm in derivative) in differentiating the bones according to their collagen content. The wavelengths around 1910-1935 nm (1891-1945 nm in derivative) that can be attributed either to the O-H bands of hydroxyapatite or to the water content in the samples, seemed to influence the dispersion of the spectra belonging to the same sample. Based on PCA results we were able to tentatively describe the bones according to their collagen content. The sample presenting the highest relative content of collagen was RP, followed by SMM and OV. Collagen was also detected in sample RB63 although probably in a lower amount. Finally, samples R313, UC86, UC88 seemed to be characterized by the lowest content of collagen. Since the characteristic collagen bands were not detected, collagen may have been present possibly in a very low amount or be even absent.

3.3 Metal samples

Although little has been done to explore the use of NIR spectroscopy for identifying corrosion products in bronze patinas, the infrared microscopy extended range of MCT detectors (7800-650 cm-1) was recently exploited to study small samples from the corrosion surface of the bronze sculpture of Neptune in Bologna [20]. In addition, SWIR imaging system (1000-2500 nm) has also been used for on-site mapping of corrosion products on two sites of a bronze sculpture of Auguste Rodin [61].

However, neither analytical approach can be easily used on-site by inexperienced operators.

Since accurately characterizing outdoor bronze patinas is fundamental in planning appropriate conservation interventions, the on-site characterization of corrosion products using our miniaturized spectrometer seems extremely promising.

Brochantite ($Cu_4SO_4(OH)_6$), antlerite ($Cu_3SO_4(OH)_4$) and atacamite ($Cu_2Cl(OH)_3$) are three copper-based corrosion products commonly found on the surface of outdoor bronze sculptures. Brochantite and antlerite typically grow on outdoor sculptures exposed in urban environments, whereas atacamite is mainly found in marine environments. These compounds indicate a proliferation of dangerous corrosion processes and thus being able to identify helps in revealing the state of conservation of the sculpture. Brochantite and antlerite are the result of electrochemical processes involving the interaction of the bronze alloy with SO_2 from the atmosphere. Atacamite is a warning signal of the presence of copper chlorides, which may be related to a dangerous and highly corrosive phenomenon called “bronze disease” [62].

The above-mentioned corrosion products can be easily identified by their characteristic absorption bands in the near infrared [20]. The spectra of the synthesised compounds, collected by means of the NIR prototype, are presented in Fig. 5a. The brochantite spectrum has a weak band at 1431 nm due to the 1st overtone of the OH stretching and a broad band at 1945 nm. Antlerite shows two well-defined bands at 1431 and 1477 nm, the former assigned to the 1st overtone of the OH stretching, and a broad band at 1968 nm. Atacamite presents several bands, the most characteristic located at 1469 (1st overtone OH stretching), 1861, 1953 (shoulder) and 1992 nm (not assigned).

Eleven spectra from each standard compound were collected and submitted to PCA. Fig. 5b shows the first derivative spectra submitted to PCA. The score plot PC1 vs PC2 (Fig. 5c) shows the well-separated compounds, while the loading plot PC1 vs PC2 highlights the relevance of the variable at 1992 nm (2007 nm in derivative) for atacamite and 1431 and 1477 nm for antlerite (1423 and 1461 nm in first derivative) as the reason for the separation.

Since the multivariate method differentiated among the three standard compounds, it was also applied to data collected from naturally-occurring corrosion products in different environments or artificially produced in the laboratory. Thus, samples presenting corrosion products grown in the urban environment (sample UN), marine environment (sample MN), and an artificial patina (sample UA) were submitted to the analysis. The spectra are reported in Fig. 6a.

Although the NIR spectrum of the UN sample is noisy, it shows a weak band at 1438 nm thus assigning the first overtone of OH stretching of brochantite. The spectrum of the UA sample shows the OH overtone at 1431 nm and a very week band at 1469 nm, revealing the presence of brochantite and, in a smaller amount, antlerite. By comparing the standard spectrum of atacamite with the MN spectrum, the signal in the first overtone region (1461 nm) as well as the strong band at 1984 nm can be linked to the presence of atacamite. XRD and FTIR data collected on the three patina samples and reported in the pertinent literature [23, 24] confirm the results obtained with the NIR prototype.

PCA analysis applied to the near infrared data led to interesting results for the differentiation of bronze patinas grown in different environments (Fig. 6c). The near infrared data of UN, MN and UA show a good separation in the score plot PC1 vs PC2 (Fig. 6c). The loading plot (Fig. 6d) highlights the important role of the variables at 1984 nm (2015 in first derivative) for the separation of MN spectra. The separation of spectra recorded on UN and UA samples, was linked to variables in the first overtone region, and also to the band at 1438 nm (1484 nm in first derivative). We believe that these results underline the usefulness of our small portable micro NIR sensor for the in-situ study of copper-based corrosion products.

4. Conclusions

We have proposed a new SWIR portable prototype (1200-2200 nm) in combination with multivariate data analysis. This can be used as an on-situ, rapid, non-invasive methodology for identifying and differentiating materials in objects of artistic and archaeological interest. Our instrument is at the cutting edge of the development of miniaturized devices. In terms of its use in the cultural heritage is concerned, the methodology managed to: i) differentiate between the materials used as a support for cinematographic film, ii) sort out archaeological bone fragments according to their collagen content, and iii) differentiate between corrosion products on outdoor bronze sculpture. The spectral range employed proved to be well suited for the analysis of the selected objects as they all presented characteristic overtone or combination bands.

We believe that the results obtained using our methodology have important implications in the study and preservation of the different materials. The differentiation of cinematographic film samples, for instance, helps conservators-restorers to safely classify the samples according to their chemical composition, thus reducing the risks connected to degradation. The identification of collagen in bone fragments means that bones can be identified according to the collagen content and thus represents an initial screening test. Finally, the presence of certain corrosion compounds on bronze sculptures may help in determining the state of conservation of the objects and consequently help in deciding whether conservation is urgently needed.

The advantages of the device in terms of cost, portability, ease of use could be exploited not only by conservation scientists but also conservators and conservator-restorers. To this aim, further efforts will be devoted to the development of new chemometric approaches for the automatic data processing and interpretation.

5. Acknowledgments

The authors would like to thank Marianna de Sanctis, Maura Pischedda and Fabiana Appicciafuoco from the “L’immagine Ritrovata”– Film Restoration Laboratory in Bologna for kindly provide the cinematographic film samples used in this research.

6. References

[1] Á. Ríos, M. Zougagh, M. Avila, Miniaturization through lab-on-a-chip: Utopia or reality for routine laboratories? A review, Anal. Chim. Acta 740 (2012) 1-11. https://doi.org/10.1016/j.aca.2012.06.024.
[2] V. Gubala, L.F. Harris, A.J. Ricco, M.X. Tan, D.E. Williams, Point of care diagnostics: Status and future, Anal. Chem. 84(2) (2012) 487-515. https://doi.org/10.1021/ac2030199.
[3] N.A. O'Brien, C.A. Hulse, D.M. Friedrich, F.J. Van Milligen, M.K. von Gunten, F. Pfeifer, H.W. Siesler, Miniature near-infrared (NIR) spectrometer engine for handheld applications, Journal 8374 (Year) 837404. https://doi.org/10.1117/12.917983.
[4] C.A. Teixeira Dos Santos, M. Lopo, R.N.M.J. Páscoa, J.A. Lopes, A review on the applications of portable near-infrared spectrometers in the agro-food industry, Appl Spectrosc 67(11) (2013) 1215-1233. https://doi.org/10.1366/13-07228.
[5] D.M. Friedrich, C.A. Hulse, M. Von Gunten, E.P. Williamson, C.G. Pederson, N.A. O'Brien, Miniature near-infrared spectrometer for point-of-use chemical analysis, Journal 8992 (Year). https://doi.org/10.1117/12.2040669.
[6] M. Alcalà, M. Blanco, D. Moyano, N.W. Broad, N. O'Brien, D. Friedrich, F. Pfeifer, H.W. Siesler, Qualitative and quantitative pharmaceutical analysis with a novel hand-held miniature near infrared spectrometer, J. Near Infrared Spectrosc. 21(6) (2013) 445-457. https://doi.org/10.1255/jnirs.1084.
[7] A. Guillemain, K. Dégardin, Y. Roggo, Performance of NIR handheld spectrometers for the detection of counterfeit tablets, Talanta 165 (2017) 632-640. https://doi.org/10.1016/j.talanta.2016.12.063.
[8] K. Tsujikawa, T. Yamamuro, K. Kuwayama, T. Kanamori, Y.T. Iwata, K. Miyamoto, F. Kasuya, H. Inoue, Application of a portable near infrared spectrometer for presumptive identification of psychoactive drugs, Forensic Sci. Int. 242 (2014) 162-171. https://doi.org/10.1016/j.forsciint.2014.05.020.
[9] M. Bacci, R. Chiari, S. Porcinai, B. Radicati, Principal component analysis of near-infrared spectra of alteration products in calcareous samples: An application to works of art, Chemometr. Intelligent Lab. Syst. 39(1) (1997) 115-121. https://doi.org/10.1016/S0169-7439(97)00063-4.
[10] M. Bacci, M. Picollo, G. Trumpy, M. Tsukada, D. Kunzelman, Non-invasive identification of white pigments on 20th-century oil paintings by using fiber optic reflectance spectroscopy, J. Am. Inst. Conserv. 46(1) (2007) 27-37. https://doi.org/10.1179/019713607806112413.
[11] J.K. Delaney, P. Ricciardi, L.D. Glinsman, M. Facini, M. Thoury, M. Palmer, E.R. De La Rie, Use of imaging spectroscopy, fiber optic reflectance spectroscopy, and X-ray fluorescence to map and identify pigments in illuminated manuscripts, Stud Conserv 59(2) (2014) 91-101. https://doi.org/10.1179/2047058412Y.0000000078.
[12] M. Aceto, A. Agostino, G. Fenoglio, A. Idone, M. Gulmini, M. Picollo, P. Ricciardi, J.K. Delaney, Characterisation of colourants on illuminated manuscripts by portable fibre optic UV-visible-NIR reflectance spectrophotometry, Analytical Methods 6(5) (2014) 1488-1500. https://doi.org/10.1039/C3AY41904E.
[13] S. Baronti, A. Casini, L. Lotti, S. Porcinai, Multispectral imaging system for the mapping of pigments in works of art by use of principal–component analysis, Appl. Opt. 37(8) (1998) 1299-1309. https://doi.org/10.1364/AO.37.001299.
[14] K.A. Dooley, S. Lomax, J.G. Zeibel, C. Miliani, P. Ricciardi, A. Hoenigswald, M. Loew, J.K. Delaney, Mapping of egg yolk and animal skin glue paint binders in Early Renaissance paintings using near infrared reflectance imaging spectroscopy, Analyst 138(17) (2013) 4838-4848. https://doi.org/10.1039/C3AN00926B.
[15] P. Ricciardi, J.K. Delaney, M. Facini, J.G. Zeibel, M. Picollo, S. Lomax, M. Loew, Near infrared reflectance imaging spectroscopy to map paint binders in situ on illuminated manuscripts, Angew. Chem. Int. Ed. 51(23) (2012) 5607-5610. https://doi.org/10.1002/anie.201200840.
[16] C. Malegori, E.J. Nascimento Marques, S.T. de Freitas, M.F. Pimentel, C. Pasquini, E. Casiraghi, Comparing the analytical performances of Micro-NIR and FT-NIR spectrometers in the

evaluation of acerola fruit quality, using PLS and SVM regression algorithms, Talanta 165 (2017) 112-116. https://doi.org/10.1016/j.talanta.2016.12.035.
[17] R. Risoluti, S. Materazzi, F. Tau, A. Russo, F.S. Romolo, Towards innovation in paper dating: a MicroNIR analytical platform and chemometrics, Analyst 143(18) (2018) 4394-4399. https://doi.org/10.1039/C8AN00871J.
[18] R. Risoluti, G. Gullifa, A. Battistini, S. Materazzi, "Lab-on-Click" Detection of Illicit Drugs in Oral Fluids by MicroNIR-Chemometrics, Anal. Chem. 91(10) (2019) 6435-6439. https://doi.org/10.1021/acs.analchem.9b00197.
[19] D.A. Burns, E.W. Ciurczak, Handbook of near-infrared analysis, CRC press2007.
[20] E. Catelli, G. Sciutto, S. Prati, Y. Jia, R. Mazzeo, Characterization of outdoor bronze monument patinas: the potentialities of near-infrared spectroscopic analysis, Environ. Sci. Pollut. Res. 25(24) (2018) 24379-24393. https://doi.org/10.1007/s11356-018-2483-3.
[21] Paints and varnishes. Artificial weathering and exposure to artificial radiation. Exposure to filtered xenon-arc radiation, EN-ISO 11341:2004.
[22] Corroion tests in artificial atmosphere. Salt spray tests, EN-ISO 9227:2006.
[23] R. Mazzeo, S. Bittner, G. Farron, R. Fontinha, D. Job, E. Joseph, P. Letardi, M. Mach, S. Prati, M. Salta, Development and evaluation of new treatments for outdoor bronze monuments, Conservation Science 2007 (2008).
[24] Development and evaluation of new treatments for the conservation-restoration of outdoor stone and bronze monuments, Activity reports 24 and 60 months for bronze - Eu-ARTECH project (2008).
[25] A. Neves, E.M. Angelin, É. Roldão, M.J. Melo, New insights into the degradation mechanism of cellulose nitrate in cinematographic films by Raman microscopy, J. Raman Spectrosc. 50(2) (2019) 202-212. https://doi.org/10.1002/jrs.5464.
[26] A. Tulsi Ram, Archival preservation of photographic films-A perspective, Polym Degradation Stab 29(1) (1990) 3-29. https://doi.org/10.1016/0141-3910(90)90019-4.
[27] M.T. Giachet, M. Schilling, K. McCormick, J. Mazurek, E. Richardson, H. Khanjian, T. Learner, Assessment of the composition and condition of animation cels made from cellulose acetate, Polym Degradation Stab 107 (2014) 223-230. https://doi.org/10.1016/j.polymdegradstab.2014.03.009.
[28] E. Ciliberto, P. Gemmellaro, V. Iannuso, S. La Delfa, R.G. Urso, E. Viscuso, Characterization and weathering of motion-picture films with support of cellulose nitrate, cellulose acetate and polyester, Procedia Chemistry 8 (2013) 175-184.
[29] I. Bonaduce, E. Ribechini, F. Modugno, M.P. Colombini, Analytical approaches based on gas chromatography mass spectrometry (GC/MS) to study organic materials in artworks and archaeological objects, Topics in Current Chemistry, Springer Verlag2016, pp. 1-37.
[30] F.C. Izzo, A. Carrieri, G. Bartolozzi, H.V. Keulen, I. Lorenzon, E. Balliana, C. Cucci, F. Grazzi, M. Picollo, Elucidating the composition and the state of conservation of nitrocellulose-based animation cells by means of non-invasive and micro-destructive techniques, Journal of Cultural Heritage 35 (2019) 254-262. https://doi.org/10.1016/j.culher.2018.09.010.
[31] V. Knotek, P. Korandová, R. Kalousková, M. Durovič, Study of triacetate cinematographic films and magnetic audio track by infrared spectroscopy, Koroze Ochr. Mater. 62(1) (2018) 26-32. https://doi.org/10.2478/kom-2018-0005.
[32] F.W. Langkilde, A. Svantesson, Identification of celluloses with Fourier-Transform (FT) mid-infrared, FT-Raman and near-infrared spectrometry, J. Pharm. Biomed. Anal. 13(4-5) (1995) 409-414. https://doi.org/10.1016/0731-7085(95)01298-Y.
[33] A. Wójciak, H. Kasprzyk, E. Sikorska, A. Krawczyk, M. Sikorski, A. Wesełucha-Birczyńska, FT-Raman, FT-infrared and NIR spectroscopic characterization of oxygen-delignified kraft pulp treated with hydrogen peroxide under acidic and alkaline conditions, Vib. Spectrosc. 71 (2014) 62-69. https://doi.org/10.1016/j.vibspec.2014.01.007.

[34] X. Li, C. Sun, B. Zhou, Y. He, Determination of Hemicellulose, Cellulose and Lignin in Moso Bamboo by Near Infrared Spectroscopy, Sci. Rep. 5 (2015). https://doi.org/10.1038/srep17210.
[35] E.W. Crandall, A.N. Jagtap, The near-infrared spectra of polymers, J. Appl. Polym. Sci. 21(2) (1977) 449-454. https://doi.org/10.1002/app.1977.070210211.
[36] C. Kradjel, K.A. Lee, NIR analysis of polymers, Handbook of Near-Infrared Analysis, CRC Press2007, pp. 547-586.
[37] J. Zhang, K. Tian, C. Lei, S. Min, Identification and quantification of microplastics in table sea salts using micro-NIR imaging methods, Analytical Methods 10(24) (2018) 2881-2887. https://doi.org/10.1039/C8AY00125A.
[38] A.D. de Oliveira, V.H. de Silva, M.F. Pimentel, G.M. Vinhas, C. Pasquini, Y.M.B.d. Almeida, Use of Infrared Spectroscopy and Near Infrared Hyperspectral Images to Evaluate Effects of Different Chemical Agents on PET Bottle Surface, Materials Research 21(5) (2018). http://orcid.org/0000-0003-1041-7144.
[39] C.E. Miller, Near-Infrared Spectroscopy of Synthetic and Industrial Samples, Handbook of vibrational spectroscopy (2006).
[40] F. Zapata, M. Ferreiro-González, C. García-Ruiz, Interpreting the near infrared region of explosives, Spectrochim. Acta Part A Mol. Biomol. Spectrosc. 204 (2018) 81-87. https://doi.org/10.1016/j.saa.2018.06.002.
[41] A.M. Senna, K.M. Novack, V.R. Botaro, Synthesis and characterization of hydrogels from cellulose acetate by esterification crosslinking with EDTA dianhydride, Carbohydr Polym 114 (2014) 260-268. https://doi.org/10.1016/j.carbpol.2014.08.017
[42] C.E. Miller, B.E. Eichinger, Determination of crystallinity and morphology of fibrous and bulk poly (ethylene terephthalate) by near-infrared diffuse reflectance spectroscopy, Appl Spectrosc 44(3) (1990) 496-504. https://doi.org/10.1366/0003702904086173.
[43] J. Yan, N. Villarreal, B. Xu, Characterization of Degradation of Cotton Cellulosic Fibers Through Near Infrared Spectroscopy, J. Polym. Environ. 21(4) (2013) 902-909. https://doi.org/10.1007/s10924-013-0605-z.
[44] A. Alassali, S. Fiore, K. Kuchta, Assessment of plastic waste materials degradation through near infrared spectroscopy, Waste Manage. 82 (2018) 71-81. https://doi.org/10.1016/j.wasman.2018.10.010..
[45] N.S. Allen, M. Edge, J.H. Appleyard, T.S. Jewitt, C.V. Horie, D. Francis, Acid-catalysed degradation of historic cellulose triacetate, cinematographic film: Influence of various film parameters, Eur Polym J 24(8) (1988) 707-712. https://doi.org/10.1080/00223638.1988.11736999.
[46] D. Littlejohn, R.A. Pethrick, A. Quye, J.M. Ballany, Investigation of the degradation of cellulose acetate museum artefacts, Polym Degradation Stab 98(1) (2013) 416-424. https://doi.org/10.1016/j.polymdegradstab.2012.08.023.
[47] S. Cersoy, S. Zirah, A. Marie, A. Zazzo, Toward a versatile protocol for radiocarbon and proteomics analysis of ancient collagen, J. Archaeol. Sci. 101 (2019) 1-10. https://doi.org/10.1016/j.jas.2018.10.009.
[48] R.E.M. Hedges, Bone diagenesis: An overview of processes, Archaeometry 44(3) (2002) 319-328. https://doi.org/10.1111/1475-4754.00064.
[49] G.J. van Klinken, Bone collagen quality indicators for palaeodietary and radiocarbon measurements, J. Archaeol. Sci. 26(6) (1999) 687-695. https://doi.org/10.1006/jasc.1998.0385.
[50] C. Kendall, A.M.H. Eriksen, I. Kontopoulos, M.J. Collins, G. Turner-Walker, Diagenesis of archaeological bone and tooth, Palaeogeogr. Palaeoclimatol. Palaeoecol. 491 (2018) 21-37. https://doi.org/10.1016/j.palaeo.2017.11.041.
[51] A. Amadasi, A. Cappella, C. Cattaneo, P. Cofrancesco, L. Cucca, D. Merli, C. Milanese, A. Pinto, A. Profumo, V. Scarpulla, E. Sguazza, Determination of the post mortem interval in skeletal remains by the comparative use of different physico-chemical methods: Are they reliable as an alternative to 14C?, HOMO 68(3) (2017) 213-221. https://doi.org/10.1016/j.jchb.2017.03.006.

[52] C.A.M. France, D.B. Thomas, C.R. Doney, O. Madden, FT-Raman spectroscopy as a method for screening collagen diagenesis in bone, J. Archaeol. Sci. 42(1) (2014) 346-355. https://doi.org/10.1016/j.jas.2013.11.020.
[53] C. Woess, S.H. Unterberger, C. Roider, M. Ritsch-Marte, N. Pemberger, J. Cemper-Kiesslich, P. Hatzer-Grubwieser, W. Parson, J.D. Pallua, Assessing various Infrared (IR) microscopic imaging techniques for post-mortem interval evaluation of human skeletal remains, PloS one 12(3) (2017) e0174552. https://doi.org/10.1371/journal.pone.0174552.
[54] G. Pothier Bouchard, S.M. Mentzer, J. Riel-Salvatore, J. Hodgkins, C.E. Miller, F. Negrino, R. Wogelius, M. Buckley, Portable FTIR for on-site screening of archaeological bone intended for ZooMS collagen fingerprint analysis, J.Archaeol. Sci. Rep. 26 (2019). https://doi.org/10.1016/j.jasrep.2019.05.027.
[55] W.J. Pestle, V. Brennan, R.L. Sierra, E.K. Smith, B.J. Vesper, G.A. Cordell, M.D. Colvard, Hand-held Raman spectroscopy as a pre-screening tool for archaeological bone, J. Archaeol. Sci. 58 (2015) 113-120. https://doi.org/10.1016/j.jas.2015.03.027.
[56] M.J. De La Haba, J.A. Fernández Pierna, O. Fumière, A. Garrido-Varo, J.E. Guerrero, D.C. Pérez-Marín, P. Dardenne, V. Baeten, Discrimination of fish bones from other animal bones in the sedimented fraction of compound feeds by near infrared microscopy, J. Near Infrared Spectrosc. 15(2) (2007) 81-88. https://doi.org/10.1255/jnirs.688.
[57] D. Baykal, O. Irrechukwu, P.C. Lin, K. Fritton, R.G. Spencer, N. Pleshko, Nondestructive assessment of engineered cartilage constructs using near-infrared spectroscopy, Appl Spectrosc 64(10) (2010) 1160-1166. https://doi.org/10.1366/000370210792973604.
[58] E.T. Stathopoulou, V. Psycharis, G.D. Chryssikos, V. Gionis, G. Theodorou, Bone diagenesis: New data from infrared spectroscopy and X-ray diffraction, Palaeogeogr. Palaeoclimatol. Palaeoecol. 266(3-4) (2008) 168-174. https://doi.org/10.1016/j.palaeo.2008.03.022.
[59] D.B. Thomas, C.M. McGoverin, A. Chinsamy, M. Manley, Near infrared analysis of fossil bone from the Western Cape of South Africa, J. Near Infrared Spectrosc. 19(3) (2011) 151-159. https://doi.org/10.1255/jnirs.926.
[60] M. Sponheimer, C.M. Ryder, H. Fewlass, E.K. Smith, W.J. Pestle, S. Talamo, Saving Old Bones: a non-destructive method for bone collagen prescreening, bioRxiv (2019) 653212. https://doi.org/10.1038/s41598-019-50443-2.
[61] E. Catelli, L. Randeberg, H. Strandberg, B. Alsberg, A. Maris, L. Vikki, Can hyperspectral imaging be used to map corrosion products on outdoor bronze sculptures?, Journal of Spectral Imaging 7(1) (2018) a1. https://doi.org/10.1255/jsi.2018.a10.
[62] D.A. Scott, Copper and bronze in art: corrosion, colorants, conservation, Getty publications2002.

Figure Captions

Fig. 1: The prototype SWIR spectrometer.

Fig. 2: Analysis of cinematographic film samples well-preserved; a) representative spectra of cinematographic film support cellulose acetate (CA), cellulose nitrate (CN) and polyethylene terephthalate (PET); b) first derivative spectra of cellulose acetate (CA), cellulose nitrate (CN) and polyethylene terephthalate (PET); c) Score plot of CA, CN and PET samples; d) loading plot of CA, CN and PET.

Fig. 3: Analysis of cinematographic film samples well-preserved and degraded; a) representative spectra of degraded cinematographic film support cellulose acetate (CA-d),cellulose nitrate (CN-d) and polyethylene terephthalate (PET-d);b) first derivative spectra of degraded cellulose acetate (CA-d),cellulose nitrate (CN-d) and polyethylene terephthalate (PET-d); c) Score plot of well-preserved and degraded CA, CN and PET samples; d) loading plot of well-preserved and degraded CA , CN and PET

Fig. 4: Analysis of bone samples; a) representative spectra of samples UC86, UC888, R313, OV, RB63,RP and SMN ;b) first derivative spectra of UC86, UC888, R313, OV, RB63,RP and SMN; c) Score plot of bone samples with convex polygons calculated for each class; d) loading plot of bone samples.

Fig. 5: Analysis of standard powder copper-based corrosion products; a) representative spectra of antlerite, atacamite and brochantite; b) first derivative spectra of antlerite, atacamite and brochantite; c) Score plot of copper-based corrosion product samples; d) loading plot of copper-based corrosion product samples.

Fig. 6: Analysis of natural and artificial copper-based corrosion products on copper or bronze substrates; a) representative spectra of copper-based corrosion products grown in urban artificial (UA), marine natural (MN) and urban natural (UN) environment. b) first derivative spectra of copper-based corrosion products of UA, MN and UN samples; c) score plot of UA, MN, UN samples; d) loading plot of UA, MN, UN samples.

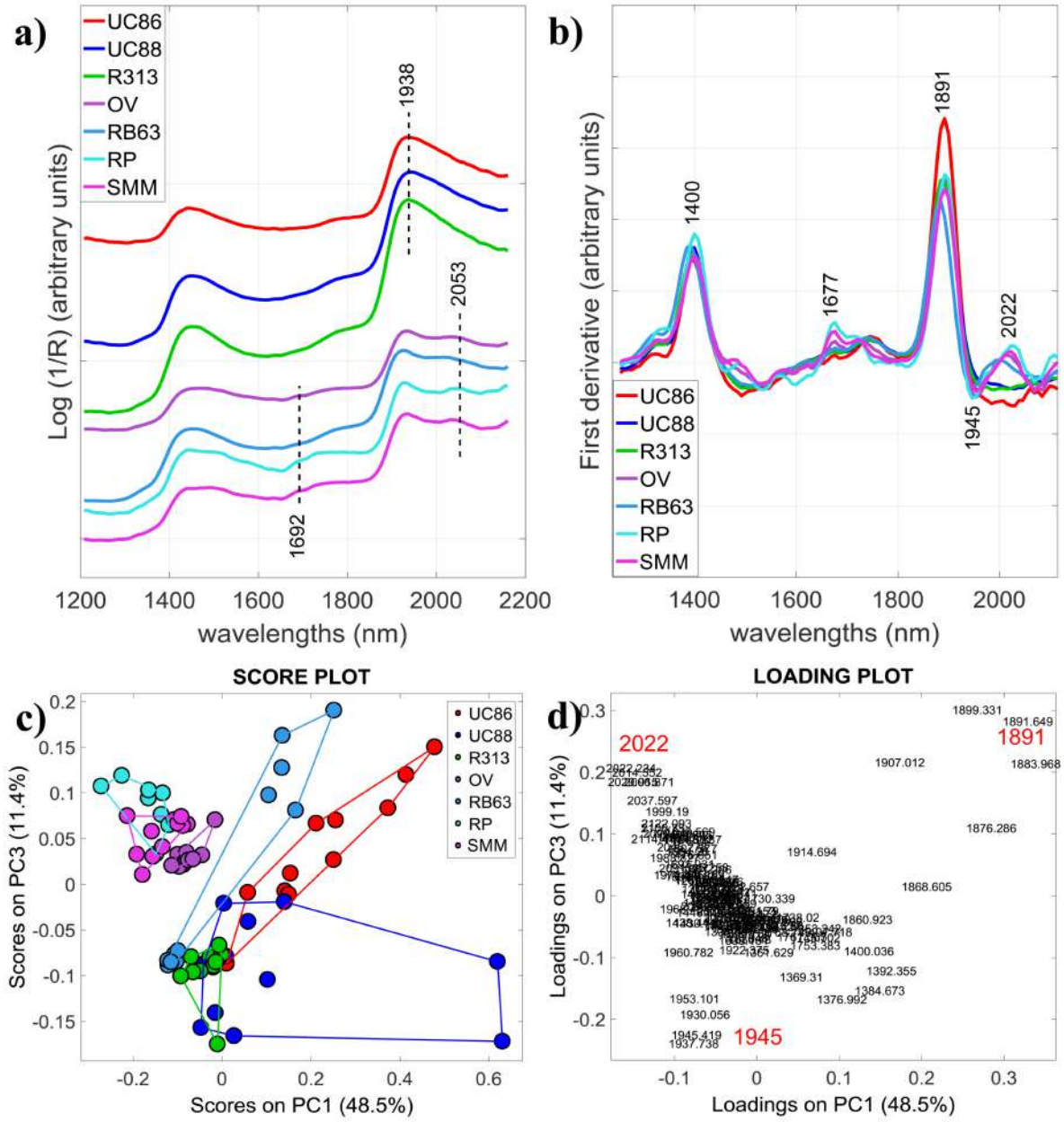
a)
UC86
UC88
R313
OV
RB63
RP
SMM
1938
2053
1692
Log (1/R) (arbitrary units)
1200
1400
1600
1800
2000
2200
wavelengths (nm)
b)
1400
1677
1891
2022
1945
First derivative (arbitrary units)
1400
1600
1800
2000
wavelengths (nm)
SCORE PLOT
c)
Scores on PC3 (11.4%)
Scores on PC1 (48.5%)
LOADING PLOT
d)
2022
1891
1945
1899.331
1891.649
1907.012
1883.968
1876.286
1914.694
1868.605
1860.923
1400.036
1392.355
1384.673
1376.992
1369.31
1960.782
1953.101
1930.056
Loadings on PC3 (11.4%)
Loadings on PC1 (48.5%)

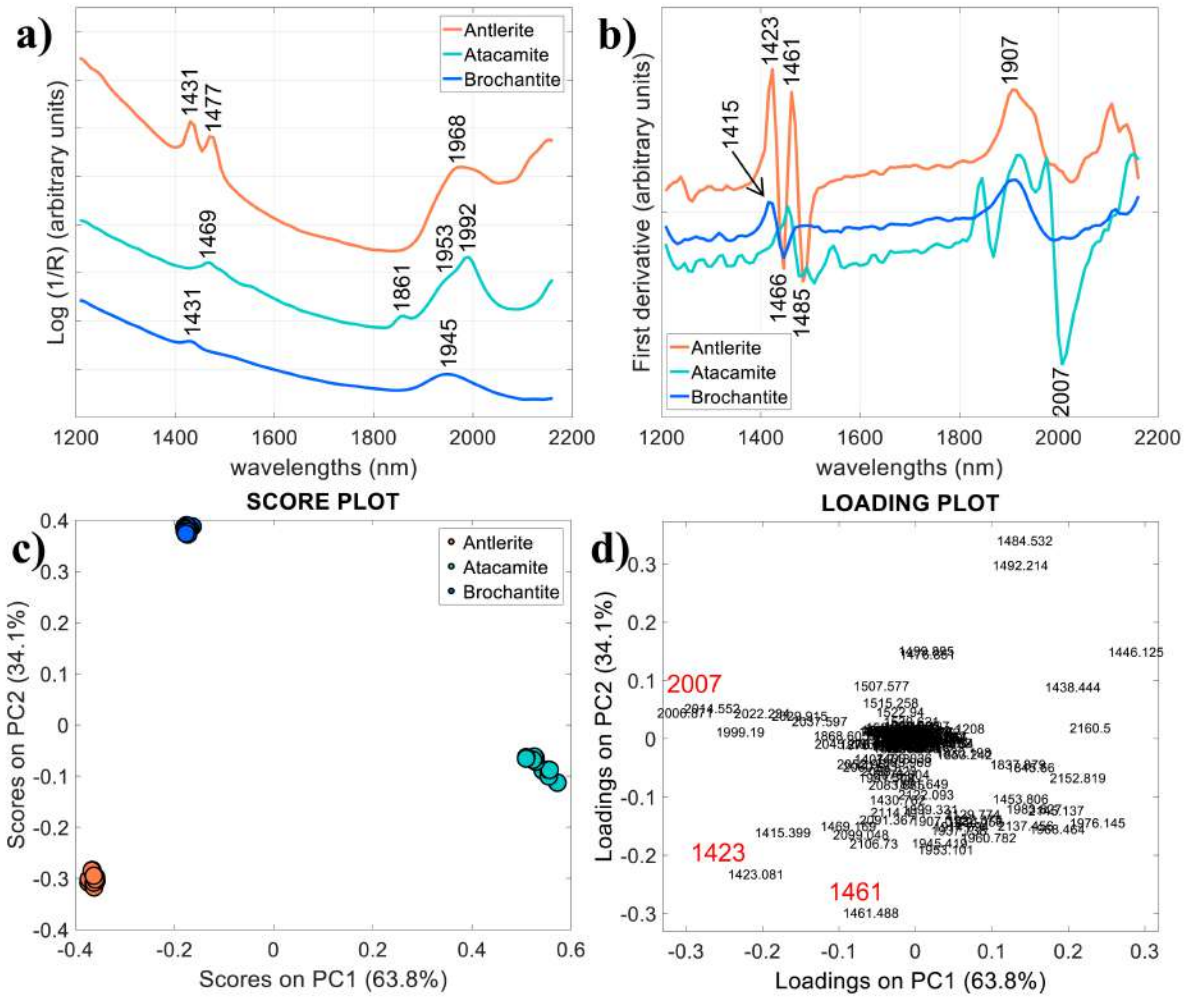
a)
Antlerite
Atacamite
Brochantite
Log (1/R) (arbitrary units)
1431
1477
1469
1431
1861
1953
1992
1968
1945
1200
1400
1600
1800
2000
2200
wavelengths (nm)
b)
First derivative (arbitrary units)
1423
1461
1415
1907
1466
1485
2007
Antlerite
Atacamite
Brochantite
wavelengths (nm)
SCORE PLOT
c)
Antlerite
Atacamite
Brochantite
Scores on PC2 (34.1%)
Scores on PC1 (63.8%)
LOADING PLOT
d)
Loadings on PC2 (34.1%)
Loadings on PC1 (63.8%)
2007
1423
1461
1484.532
1492.214
1446.125
1438.444
1507.577
1515.258
1999.19
2160.5
2152.819
1453.806
1976.145
1415.399
1423.081
1461.488

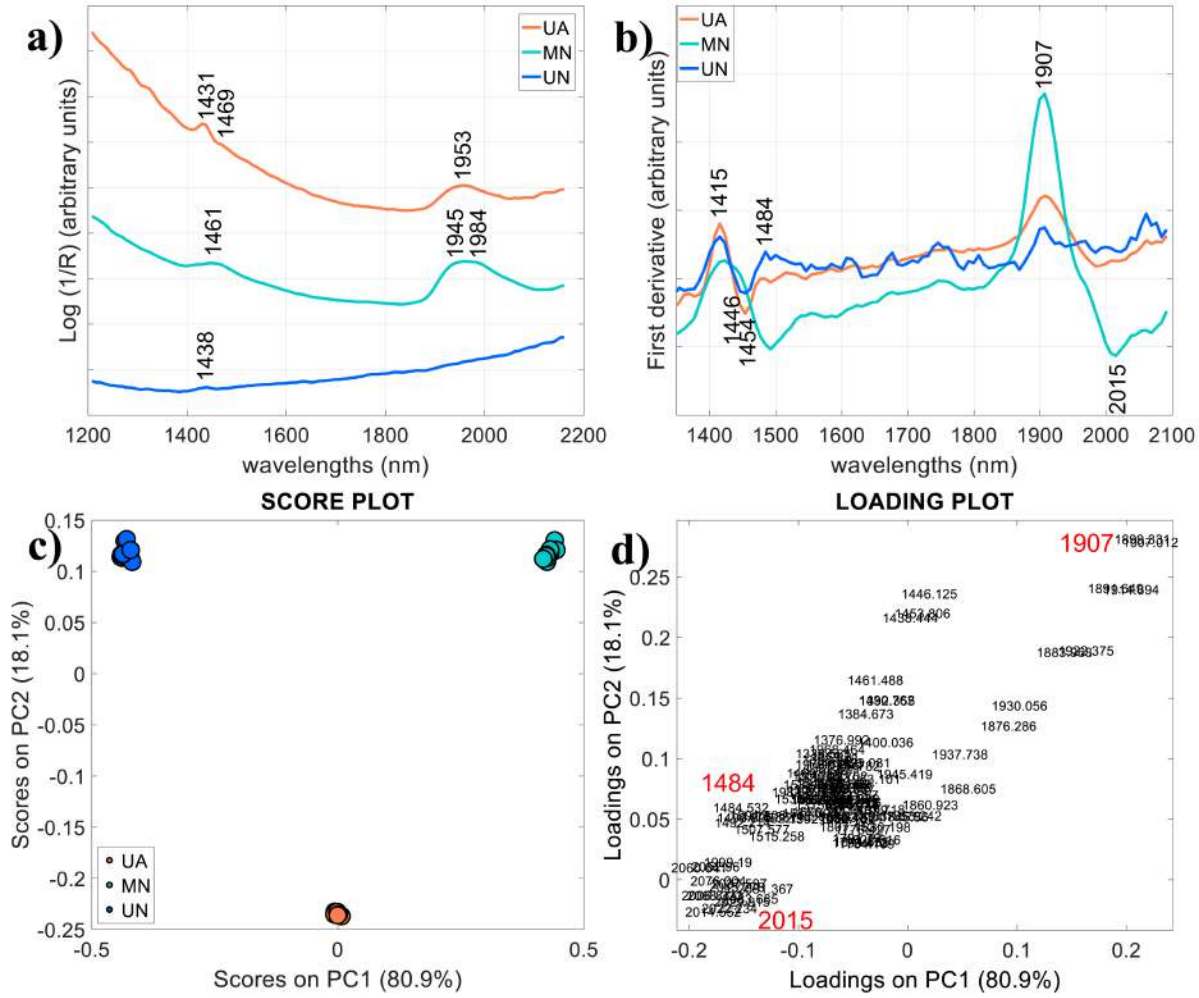
a)
UA
MN
UN
1431
1469
1953
1461
1945
1984
1438
Log (1/R) (arbitrary units)
1200
1400
1600
1800
2000
2200
wavelengths (nm)
b)
UA
MN
UN
1907
1415
1484
1446
1454
2015
First derivative (arbitrary units)
1400
1500
1600
1700
1800
1900
2000
2100
wavelengths (nm)
SCORE PLOT
c)
UA
MN
UN
Scores on PC2 (18.1%)
Scores on PC1 (80.9%)
LOADING PLOT
d)
1907
1446.125
1461.488
1384.673
1930.056
1876.286
1937.738
1484
1868.605
1860.923
2015
Loadings on PC2 (18.1%)
Loadings on PC1 (80.9%)

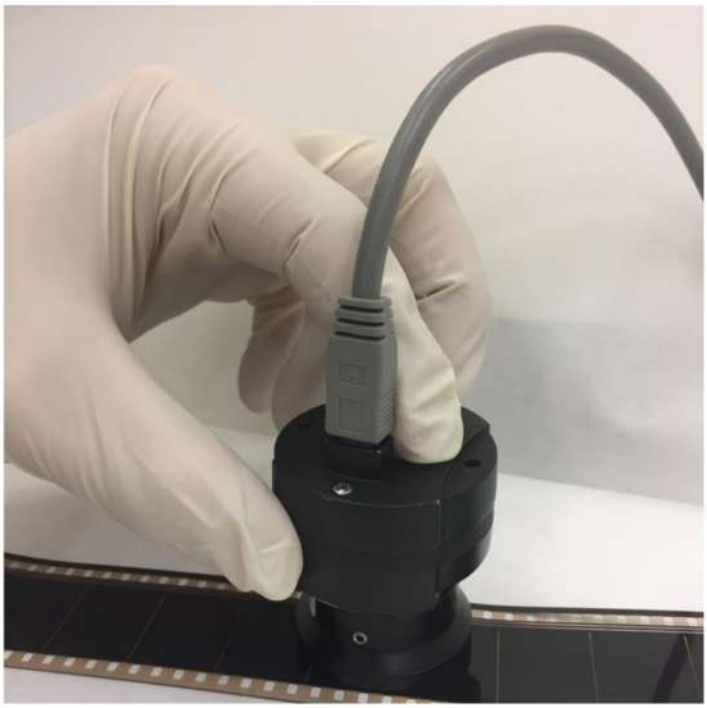

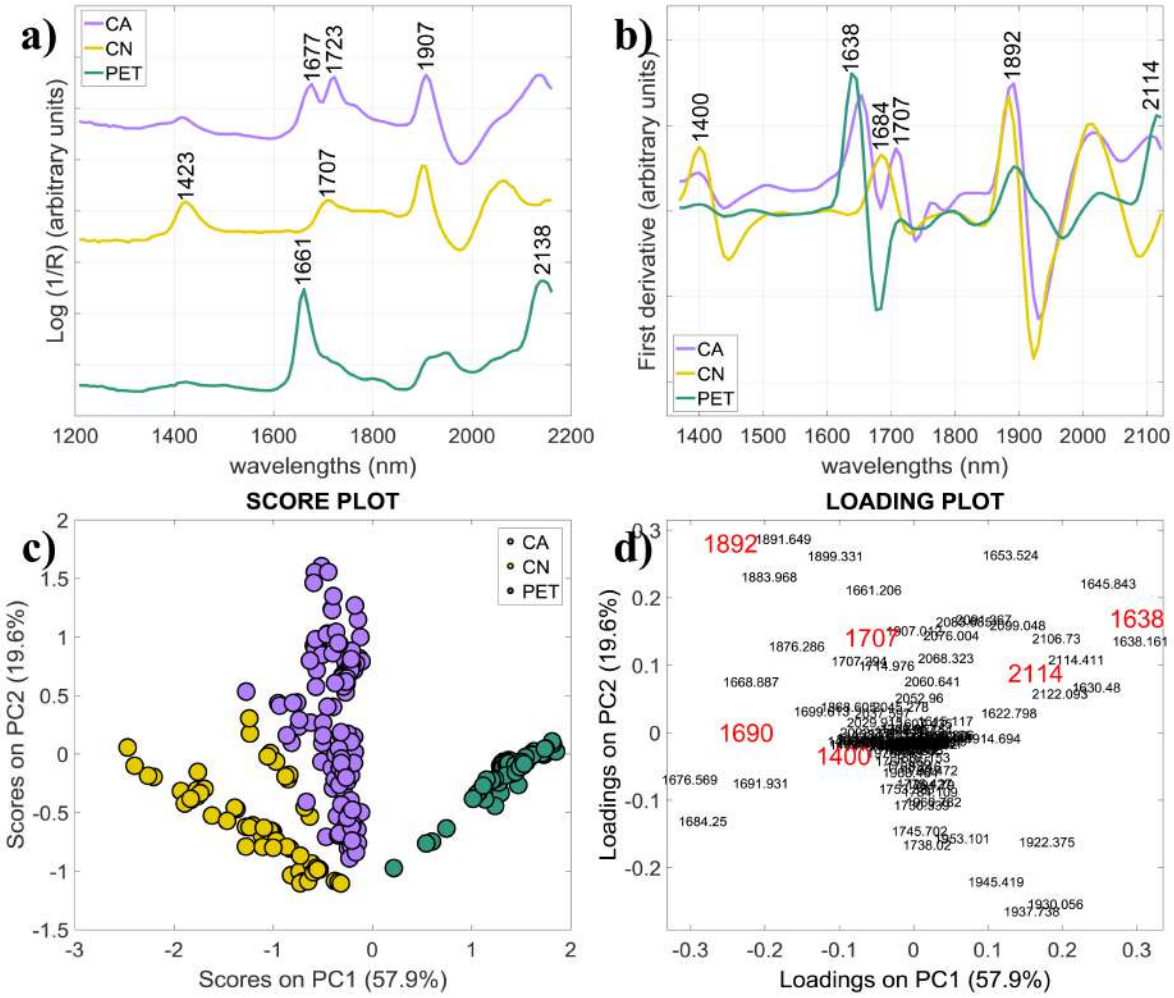
a)
CA
CN
PET
1677
1723
1907
1423
1707
1661
2138
Log (1/R) (arbitrary units)
1200
1400
1600
1800
2000
2200
wavelengths (nm)
b)
1638
1892
2114
1400
1684
1707
First derivative (arbitrary units)
CA
CN
PET
1400
1500
1600
1700
1800
1900
2000
2100
wavelengths (nm)
SCORE PLOT
c)
CA
CN
PET
Scores on PC2 (19.6%)
Scores on PC1 (57.9%)
LOADING PLOT
d)
1892
1638
1707
2114
1690
1400
Loadings on PC2 (19.6%)
Loadings on PC1 (57.9%)

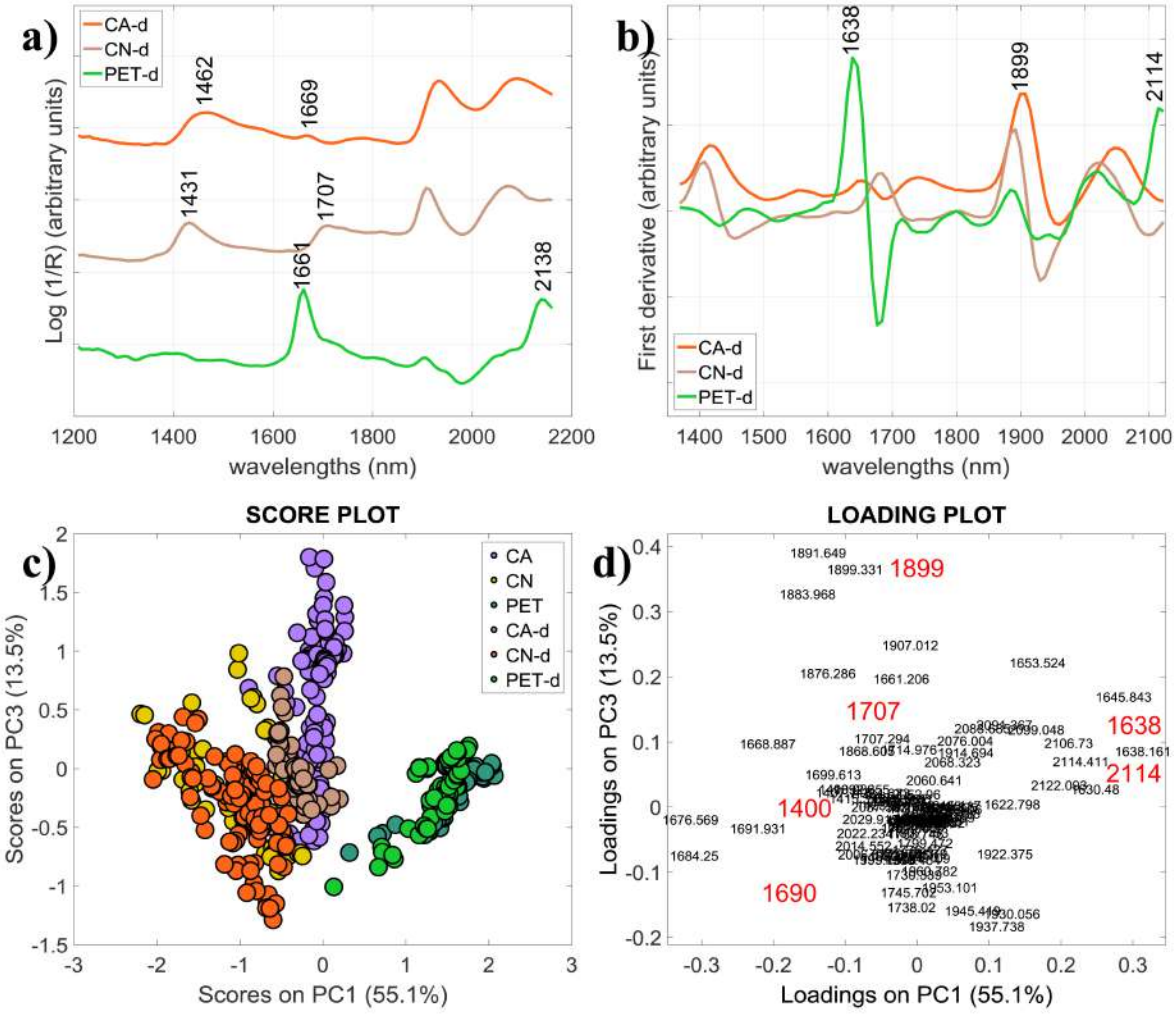
a)
CA-d
CN-d
PET-d
1462
1669
1431
1707
1661
2138
Log (1/R) (arbitrary units)
wavelengths (nm)
b)
1638
1899
2114
First derivative (arbitrary units)
wavelengths (nm)
c)
SCORE PLOT
CA
CN
PET
CA-d
CN-d
PET-d
Scores on PC3 (13.5%)
Scores on PC1 (55.1%)
d)
LOADING PLOT
1899
1707
1638
2114
1400
1690
Loadings on PC3 (13.5%)
Loadings on PC1 (55.1%)

- A new miniaturized SWIR spectrometer is proposed for cultural heritage analyses
- The prototype enables rapid information acquisition to guide restoration strategies
- The prototype can be used as an in-situ, rapid, non-invasive analytical method
- Cinematographic films, bones and bronze patinas were efficiently characterised

Declaration of interests

☒ The authors declare that they have no known competing financial interests or personal relationships that could have appeared to influence the work reported in this paper.

☐The authors declare the following financial interests/personal relationships which may be considered as potential competing interests: